MP1 - Photoplethysmographic Imaging for the Evaluation of Peripheral Blood Perfusion in a Clinical Setting

Supervised by Terence Leung & Judith Meek

Word count: 4984

Ben K. Margetts

Abstract

The ability to provide non-contact monitoring of blood perfusion, in patients susceptible to diseases such as diabetic foot, is exceptionally useful in a clinical setting. Recently, this has become achievable through a widely-used technique known as photoplethysmography. After extensively reviewing the literature on clinical applications for photoplethysymography, we began to explore the potential for objectively identifying central points of perfusion within tissue, by attempting to fit a variety of distributions to a photoplethysmography dataset. Due to the inherent noise in the data, this approach proved ineffective and so we reduced the noise in the data by utilising a three-by-three pixel neighbourhood outlier filtering technique, which was effective. A photoplethysmography blood perfusion monitoring technique was then applied to a patient with diabetes. This dataset highlighted the issues of movement artefacts to us, as the photoplethysmography results were severely perturbed by the patient's involuntary foot tremor.

1 Introduction & literature review

In clinical settings, there is a strong need for efficient, non-contact techniques for the long-term monitoring of health indices such as peripheral blood perfusion, blood flow, and vital signs. This need is especially great in patients with diabetes, where poor monitoring of peripheral blood flow can lead to conditions such as diabetic foot, where the loss of sensory information from the foot causes a lack of safeguarding against accidental self-inflicted trauma to the region [1]. In this paper we will discuss the application of a well known technique, photoplethysmography (PPG), to the monitoring of these health indices, with a focus on the assessment of peripheral blood perfusion in diabetes sufferers. This paper will open with a literature review of PPG techniques and applications within a clinical setting, and will then progress to evaluating methods by which this technique can be improved, and applied to a specific patient.

1.1 What is photoplethysmography?

Photoplethysmography is a tool for measuring changes in volume within a system where the plethysmograph is obtained through some sort of optical instrument, usually a commercially available digital camera or pulse oximeter. The technique itself has many advantages over similar investigative techniques in that it is simple to set up, low-cost, and efficient [2]. Although it has many applications across the physical and biological sciences, for the purposes of this investigation, we will focus on the application of PPG imaging to the monitoring of volumetric changes in surface and subsurface vasculature, where the absorptive nature of haemoglobin in the visible and near-infrared spectrums is utilised to monitor blood perfusion and extract vital signs [3]. As a rule of thumb, the distance between these vessels and the epidermis, along with their size, and therefore their blood carrying capacity, is proportional to the light reflected & refracted from them to the epidermal surface. This variation in emitted light takes on a regular waveform structure and produces a dampened representative trace of the cardiac cycle [4].

1.2 Contact-based photoplethysmography for monitoring vital signs

The most common use for PPG in a clinical capacity, is currently the extraction of patient vital signs. The vital signs that can be extracted from a PPG recording include a patients blood oxygen saturation, heart rate, blood pressure, stroke volume and respiration rate. To begin with, the extraction of a patient's blood oxygen saturation (SpO_2) first became widespread in the early 1990s when a form of PPG measurement, pulse oximetry, became a mandated international standard for monitoring vital signs while a patient is under anaesthesia [5]. This contact based measurement is obtained through the rapid switching of red and near-infrared wavelengths being shone through vascularised tissue. The amplitudes of the pulsatile (AC) component of these wavelengths are highly sensitive to the differences in absorption between deoxygenated haemoglobin (Hb) and oxygenated haemoglobin (HbO_2), and so from the amplitudes of the AC component of these two wavelength measurements, an estimation of SpO_2 can be calculated as a percentage of HbO_2 [6]. An accurate pulse oximetry reading can be taken from a variety of vascularised locations including extremities such as the fingers and toes, the palm of the hand, the oesophagous, the sole of the foot, the ear, and the genitals [7, 8]. Following this, an estimate of heart rate can also be extracted with a pulse oximeter, and is often displayed alongside the SpO_2 reading. Here the AC component of the PPG reading is analysed to extract the frequency at which the pulsatile component repeats itself [9]. This is then used to calculate the heart rate, and is frequently utilised in a variety of settings [4], even given that the technique is sensitive to movement artefacts and abnormalities in the frequency of the pulsatile component. For example, the confidence in a pulse oximetry reading is significantly reduced in patients with cardiac arrhythmia [10].

Another use for the PPG pulse oximeter includes the monitoring of blood pressure. This technique is not as widely utilised as the monitoring of SpO_2 and heart rate, as a traditional blood pressure inflation system that monitors differences in pressure within the cuff, is generally easier to analyse, and involves less set-up. Having said this, the use of PPG to monitor blood pressure can reveal interesting details that are absent from a standard blood pressure reading, and most importantly, moves towards contact-based technology that allows for continuous measurements to be taken [11]. There are two key methodologies by which a PPG blood pressure reading can be taken, cuff-based PPG AC waveform analysis, and surrogate pulse measures of blood pressure. Cuff-based PPG techniques are similar to those utilised in commercially-available cuff-based blood pressure systems, with the difference being the inclusion of a PPG sensor built into the cuff. This cuff is placed above the area of interest, restricting blood flow through the tissue, and monitoring the absorption/reflection of rapidly alternating red and near infrared wavelengths during arterial unloading [12]. The second methodology by which a blood pressure reading can be taken, shows far more promise in terms of allowing for non-constrained continuous measurements that the traditional cuff-based systems restrict. These surrogate pulse measurements of blood pressure utilise PPG readings alongside electrocardiography (ECG) measurements, monitoring the pulse transit time (PTT) interval between an R-wave being detected by the ECG, and the corresponding PPG AC signal being detected [13]. This information, along with the knowledge of the distance required for that pressure wave to reach the PPG sensor, is then used to produce an estimate of the blood pressure.

Another health measurement related to blood pressure, stroke volume, may also be estimated using PPG waveforms, although this is controversial within the literature base [14]. This area of research is still developing, however it appears as though the area of pulse contour amplitudes and the PTT can be used to estimate a patient's stroke volume [4]. Other attempts at deriving stroke volume with PPG measurements include using peripheral pressure volume loops from intra-arterial catheters alongside the PPG waveform [15], and use of the pressure recording analytical method (PRAM) [16, 17]. Lastly, respiratory modulations can also be extracted from the PPG waveform and used to compute a reasonably accurate respiration rate [18]. Some issues present with this type of vital sign monitoring when the subject exhibits variation from the physiological norm, i.e. yawning, gasping or vasoconstriction, with this technique also exhibiting sensitivity to movement artefacts [19].

1.3 Non-contact photoplethysmography for monitoring vital signs

A key advancement in the last few years has been the movement towards monitoring vital signs using non-contact PPG methodologies, where a video camera placed within 2 meters of the subject is used to estimate their SpO_2 levels, heart rate, and potentially their respiration rate. Non-contact monitoring represents a significant and fundamental advancement in clinical methods for monitoring vital signs. Traditional methods, including those discussed previously, require pieces of equipment to be attached to the patient, preventing hassle-free long term monitoring and causing frequent motion artefact-based false alarms. Non-contact video-based PPG is also no stranger to motion based artefacts, however with this technology, the information being received by the camera can be used to detect movement independently of the PPG waveform, and therefore adjust for the movement artefacts it introduces [20].

The first mention of non-contact PPG in the literature was in 2005 where a group discussed extracting PPG signals from a CMOS camera directed at the subject's wrist [21]. These signals were all described as containing a pulsatile component, and represented the first step towards obtaining PPG measurements from a video camera. This technology was further established in 2007 when a group attempted to produce non-contact PPG recordings via a CMOS camera directed at the subject's inner arm, with a set of LEDs illuminating the area at 760 and 880nm wavelengths, allowing for two multiplexed PPG waveforms to be simultaneously captured [22]. Both of these initial studies focused on establishing the feasibility of estimating SpO_2 readings from the non-contact recordings, however neither papers display any specific SpO_2 results, and the focus of this technology quickly shifted into other areas of vital sign monitoring.

In 2008, a landmark paper demonstrated the feasibility of extracting non-contact PPG signals from human skin, with only ambient lighting, a mid-tier digital camera, and a standard computer to produce an estimation of the subject's heart and respiration rates. This paper is the first that we are aware of to document the use of the fast Fourier transform (FFT) algorithm to extract the heart rate from the mixed frequency content of the video, and also appears to be the first to introduce the idea of pushing this technique into a clinical setting by suggesting the potential use of remote PPG imaging for characterising vascular skin lesions alongside the extraction of vital signs [23]. Following this publication, several other papers were published in 2009 exploring the potential of this technique for extracting a subjects biometric data [24], including a patent for a device that capitalised on the techniques potential for extracting vital signs. In 2010 and 2011, a series of papers from Poh et al began to examine the feasibility of using a standard webcam built into their laptops, to extract PPG recordings from volunteers of differing skin colour [25, 26]. These papers also applied the FFT algorithm to extract the pulsatile component of the PPG readings, and successfully attempted to estimate the volunteers respiration rate with a preexisting method, using indirect calculations from the measurement of a subject's heart rate variability [27]. In a similar fashion to studies mentioned previously, these papers explored the feasibility of using ambient light in the environment to extract this signal with consumer-level equipment. This idea was further explored by a plethora of papers that have explored the idea of extracting the PPG waveform with entry-level technology including a variety of digital cameras [28], mobile phone cameras [29], tablets [30], and webcams [31].

More recently, the use of non-contact PPG imaging to extract vital signs has been explored in several clinical settings, including a dialysis unit, where autoregressive models were used to cancel out artificial light flicker for continuous vital sign monitoring [32]. Lastly, a notable paper was recently published in-which remote PPG imaging was used for monitoring neonates in an intensive care unit [33]. We could provide many more examples for the use of non-contact PPG imaging in monitoring vital signs, but suffice to say, the technique has gained a large amount of traction in recent years. Current efforts in the field are aimed at reducing movement artefacts in the output, extracting the PPG pulsatile wave from the video, and better understanding what that waveform can tell us about a subject's vital signs. This is not the only use for non-contact PPG imaging however, and next we will discuss the potential for utilising PPG imaging to observe blood perfusion patterns.

1.4 Photoplethysmography for observing blood perfusion patterns

Another key emerging use for non-contact PPG imaging technology is the monitoring of surface and subsurface blood perfusion in healthy and diseased patients. With this technology, a video camera is used to monitor the change in pixel colour across human skin over time. The first mention of this in the literature appears to be in 2005, where a contact based PPG set-up of green and near-infrared light is used to examine blood perfusion in muscle. Although this is not a non-contact set-up, it is an early example of the technologies use for non-invasive investigations of blood perfusion in both skin and muscle [34]. The first non-contact set-ups investigating blood perfusion began to emerge in 2007, after the feasibility of non-contact PPG became established between 2005 and 2009. One paper by Rubins et al describes how the light intensity for each pixel of the video is monitored over time, with noise greater than 15 Hz removed, and the original video being reconstructed into a separate video that demonstrates the difference in light intensity changes from pixel to pixel, therefore extracting surface blood perfusion from the body in Sun light [35]. The second paper on this topic that was published in 2009, focused on remotely measuring blood perfusion across the human face. In this study, a CMOS camera was used to measure blood perfusion with the addition of an RCLED ring light source. This data was compared with a traditional pulse oximeter, demonstrating that the results obtained via the non-contact set-up were comparable with those obtained via pulse oximetery [36]. A follow up paper by Rubins et al in 2010 demonstrated a two dimensional mapping of blood perfusion across human fingers and face, and did this with a novel piece of image processing software, which also revealed that the green channel in an RGB image appears to be most sensitive to blood perfusion [37].

Following these developments, this topic began to receive media interest in 2013 after MIT published an open source piece of software that used a similar principle to reveal hidden features in a video, including blood perfusion across a subject's skin [38]. This was quickly followed by a clinical trial that investigated microvascular blood flow in the legs of patients with diabetes using a contact-based PPG device [39], and although interesting, to our knowledge, this has not been attempted with a non-contact PPG extraction technique. Lastly, two papers were published in 2013 and 2014 respectively, again demonstrating the feasibility of this technique for examining blood perfusion patterns in human subjects. The first paper examined blood perfusion patterns in migraine sufferers, and revealed an intriguing asynchronous blood perfusion pattern that is not present in their healthy counterparts [40]. This shows the strength and power of this relatively simple monitoring technique that was further reinforced by the 2014 paper, where the authors effectively discuss and demonstrate the use of non-contact PPG and infrared imaging to continuously monitor body temperature and blood perfusion across large sections of skin [41].

As shown in the literature, the most promising clinical PPG applications still remain with contact-based PPG techniques. In this study we will attempt to shift this outlook by improving non-contact PPG measurements and analysis with image post-processing methods. These methods will then be trialled on a video recording taken of the foot of a diabetic patient.

2 Methods

2.1 Materials and set-up

Two image capture tools were used in this study, the inbuilt camera in the iPhone 6 (Apple inc, USA), and the GoPro HERO (GoPro, USA). Both devices provide video shooting at a resolution of 1920x1080 pixels, at 30 frames per second (fps) and 60 fps respectively. Lighting used in the recordings was predominantly artificial office lighting or ambient lighting, dependent on the setting it was taken in. Where possible, automatic image correction in the devices, such as image stabilisation and automatic high dynamic range capture, was disabled to avoid interfering with the raw output. Videos were taken within 2 meters of the skin surface, with the camera physically stabilised to reduce movement artefacts. The videos were saved as .MOV files, stored and then transferred to an iMac (Apple inc, USA), where analysis was conducted. Video analysis, vital sign analysis, and PPG extraction were all conducted in the MATLAB 2014b software framework (Mathworks, USA) using custom scripts. Open

source MATLAB toolboxes [42] and [43] were used with some of our data processing tools.

2.2 Video preprocessing, downsampling, and phase mapping

The red (R), green (G), and blue (B) channels of the colour RGB videos were read into the MATLAB workspace frame-by-frame, providing a series of pixel values (PV) where PV stores the vector $PV(x, y, t)$. Here x and y give the horizontal and vertical position of the pixel within two dimensional space, and t gives the time relative to the fps value for the video. A downsampling factor of 5 was used when reading in the videos to reduce the size of the image and highlight the PPG signal differences, if any, across the surface of the skin.

The green channel of the video, having been shown to best demonstrate blood perfusion, was then extracted and projected onto a grid, where the average PV was calculated for each pixel across time. $PV(t)$ was then Fourier transformed at the user-determined heart rate frequency, producing a phase map for the grid at the frequency of interest, detailing the angle of the phase shift for each downsampled pixel in the image. A power map was also computed from the grid, displaying the power at that specific frequency of interest for each pixel.

2.3 Determining heart rate frequency

To determine the heart rate frequency of the participant, the amplitude and phase of specific pixels of interest, i.e. pixels in highly vascular regions, were plotted. The frequency of the plotted oscillatory components were then manually analysed, along with their amplitudes, to pick out the heart rate frequency. As shown in figure 1, one of the highest peaks also corresponds with a likely frequency range for the cardiac cycle, where 1.2 Hz = 72 beats per minute (bpm).

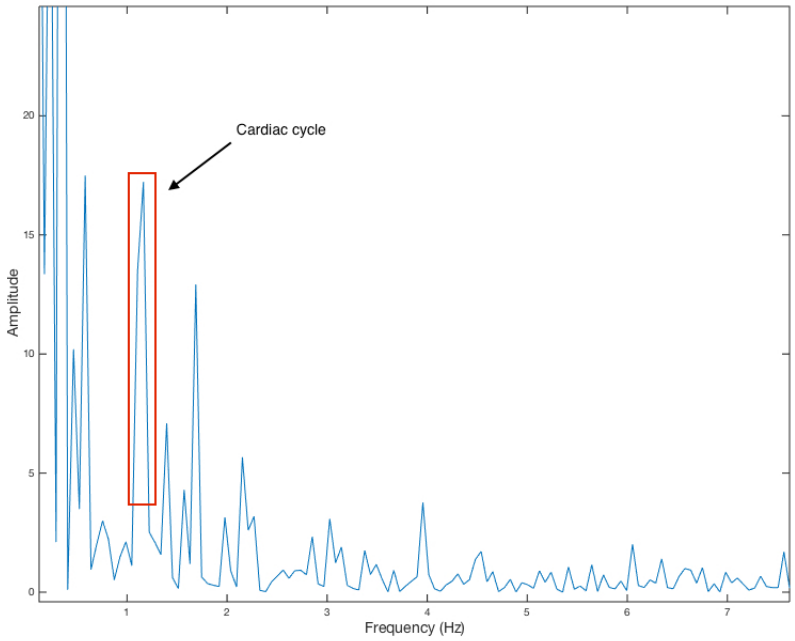

Figure 1: The frequency of oscillating components, against their amplitudes.

A normal heart beat for a healthy person falls somewhere in the range of 60-100 bpm, although this can be slightly lower for athletes, and slightly higher if the participant is not at rest. The manually selected heart rate frequency is further validated when the blood perfusion is visualised across the skin. If an incorrect heart rate frequency is selected, the video will likely display a uniform distribution of noise across the skin, rather than blood perfusion.

2.4 Monitoring blood perfusion

In order to monitor blood perfusion, the angle of the phase shift for the oscillations around the heart rate frequency are ordered for each pixel from $-\pi$ to π. These are stored along with the intensity of the heart rate frequency at that particular phase value for that specific pixel in z, producing a vector $PV(x, y, z)$ for each pixel at each value in the phase shift. These vectors are then reconstructed into an image, with one image for each step of the phase shift. Following this, the images are put into a video in order of the phase value, with a user determined factor n, determining the amount of frames that a pixel remains on the screen for, at its given intensity value, from the frame at which it was introduced. The intensity of the pixels is then converted into a scalebar from blue to red, with blue displaying very little pulse in the pixel, and red displaying the highest amount of pulsation. These values are then incorporated into the frames, where it is then written to an AVI file, with a comparative greyscale representation displaying blood perfusion in red above the blood perfusion phase map video, as can be seen in figure 2.

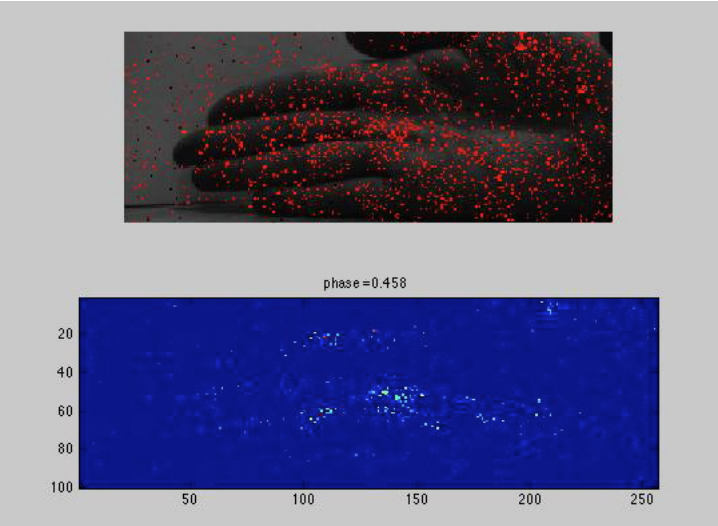

Figure 2: Example of a blood perfusion video file, with the greyscale video (top) and the blood perfusion phase map video (bottom).

2.5 Fitting a distribution to blood perfusion patterns

One approach to analysing the pattern of blood perfusion in a patient, would be to calculate 'origin points' for the perfusion patterns across the phase shift. This is possible to do through observing the output video and determining by eye, potential origins of perfusion based upon the intensity of the pixels and their distribution pattern. The issue with this analysis strategy is that it is an inherently subjective way of assessing this indicie. A novel objective method that we tested in this study, was to see how a variety of ditributions fit subsets of the data. This was accomplished by building a program that took a three-by-three matrix of the phase map, attempted to fit a variety of parametric distributions to the dataset, and then used a series of goodness of fit measurements to determine which distribution best fit the matrix. The goodness of fit measurements used to determine the best distributions for the matrix, were the negative log likelihood, the bayesian inference criteria, the akike information criteria, and the size corrected akike information criteria, in order of their importance to the weighting of the goodness of fit measurement. This weighting was then used to order the distributions fitted to the data subsets, in order of how well they fit the data. If it was found that the subset was best fit by a two-dimensional normal distribution function, then the program would perform a modified version of the one-sample Kolmogorov-Smirnov test. This modified version, known as the multivariate Kolmogorov-Smirnov test of goodness of fit [44], appeared to be the most objective measure we had for analysing the goodness of fit for a normal distribution to our dataset. The program would then record the output of this test, before moving to the next pixel in the grid, taking the 8 nearest pixels, and running the distribution fits again. When the program reached the end of the image, it would

restart, taking a larger subset of the matrix this time, i.e. a three-by-three matrix would become a four-by-four matrix that combed through the image. This program would repeat until the matrix was as large as the image would allow for in $PV(x, y)$.

The reason for our interest in fitting normal distributions to the dataset, was that if you were to picture the intensity distribution of a series of pixels, monitoring blood flowing from a central point of highly vascularised tissue into the locations around it, the most plausible scenario would be that the blood would perfuse into all surrounding locations in the immediate vicinity of the vascular network, hence resembling a two-dimensional normal distribution in the image.

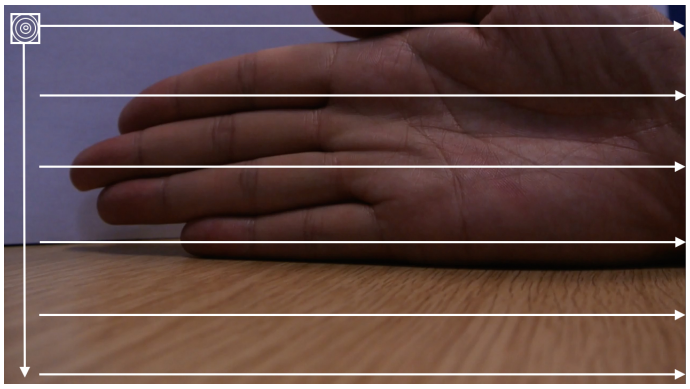

Figure 3: Example of program function.

2.6 Reducing image noise using an outlier filtering algorithm

Another issue with the PPG technique, that we sought to address through image post-processing, was the quantity of outliers in the blood perfusion video output. Within these videos, outliers in phase arise due to the cyclical nature of the phase shift, where the boundary values of $-\pi$ and π don't represent extreme differences in shift, but instead are very close in value, as the value of π is directly followed by $-\pi$. For example, if x represents the phase value of the median cardiac frequency for all pixels in the image, then the phase shift boundaries can be given be the equation.

$$f(x) = f(x \pm \pi)$$

To filter outliers, we wrote a program where a 'nearest neighbours' approach was taken to analysing each pixel in the phase plane. The program would take the phase value of the centre pixel, and the values of the 8 surrounding pixels. If the 8 surrounding pixels all held a similar value within a tolerance range of 0.2, and the centre pixel differed significantly from this value, then the mean of the pixels is calculated and given as the value for the centre pixel. This technique is often referred to as conservative smoothing, and can given by the following equation [45]:

$$PV(x,y) = 1/M \sum_{k=x-1}^{x+1} \sum_{l=y-1}^{y+1} f(k,l)$$

$$where$$

$$T_{Lower} \leq PV(x,y) \leq T_{Upper}$$

where M is the neighbourhood size, and T is the tolerance limit. A visual representation of this is given in figure 4.

Figure 4: Visualisation of outlier filtering technique.

3 Results

3.1 Extracting vital signs

Videos of the hand from two healthy volunteers were used to test the feasibility of vital sign extraction using PPG techniques. The first video was 1920x1080 pixels in size, 40 seconds in length and recorded at 30 fps. The second video was also 1920x1080 pixels in size, but was 17 seconds long, and recorded at 60 fps.

From these simple videos, both heart rates and respiration rates of the volunteers could be estimated with varying levels of confidence. In participant 1, their heart rate oscillated at a frequency of 1.2 Hz, giving a heart rate of 72 bpm; and in participant 2, their heart rate was located at a frequency of 1.1 Hz, giving an estimated heart rate of 66 bpm. In participant 1 their respiration rate was 0.21 Hz, giving an estimated respiration rate of 12.6 breaths per minute; and in participant 2, their respiration rate was more difficult to predict, with an estimation of 0.18 Hz collected from a number of locations, giving a respiration rate of 10.8 breaths per minute. This is demonstrated in figure 5 where both oscillating frequencies can be seen together in the same pixel. More distinct traces of the respiration rate are available when the two readings are collected from separate pixels.

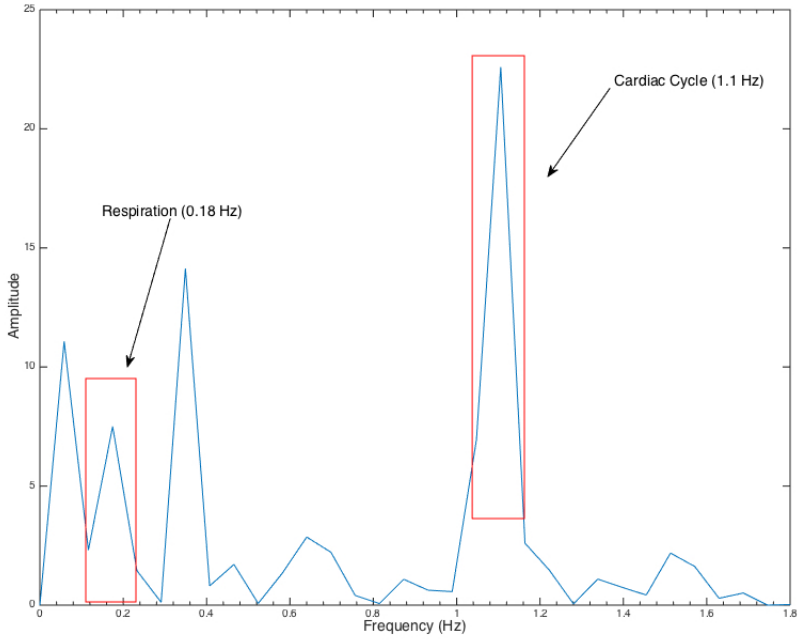

Figure 5: Heart and respiration rate estimates from a single pixel in the phase plane.

3.2 Fitting a distribution to blood perfusion patterns

This technique was trialled on videos of the hand from two healthy volunteers. The program successfully extracted multiple normally-distributed 3-by-3 matrices at positions that appeared to be central points of perfusion. Disappointingly, when these data points were submitted to the multivariate

Kolmogorov-Smirnov test for validation, the test rejected the null-hypothesis that the data fits a normal distribution at the 5% significance level.

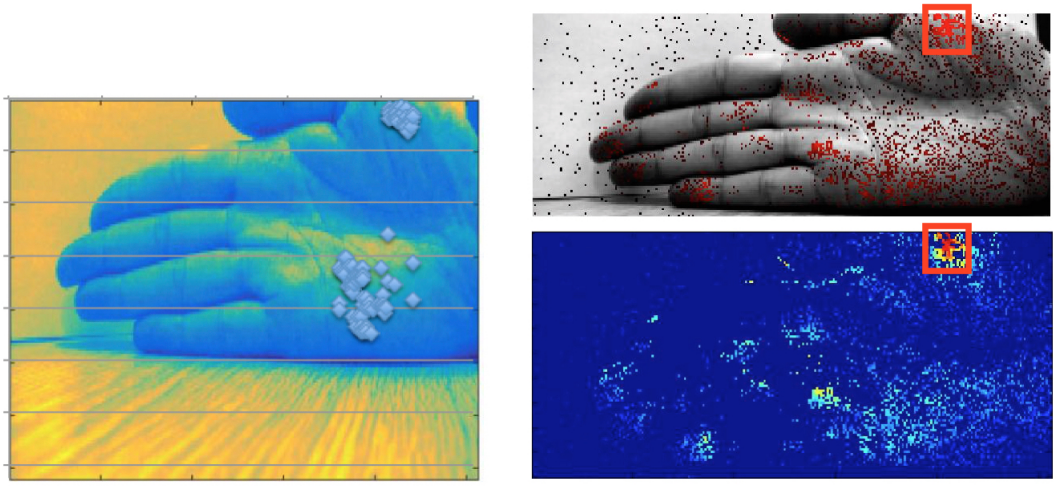

Figure 6: (Left) 3-by-3 matrix locations, plotted over a down sampled colour map of the raw video file, displaying where the data was best fit by a 2-dimensional normal distribution. (Right) Comparative frame from the blood perfusion video displaying central perfusion region of interest in red.

When these matrices are examined, it is clear that they are not normally distributed, but instead, simply best fit that distribution over other tested parametric distributions. This can be seen in figure 7, where a 'normally distributed' 3-by-3 matix is examined alongside the matrix for the entire region of interest.

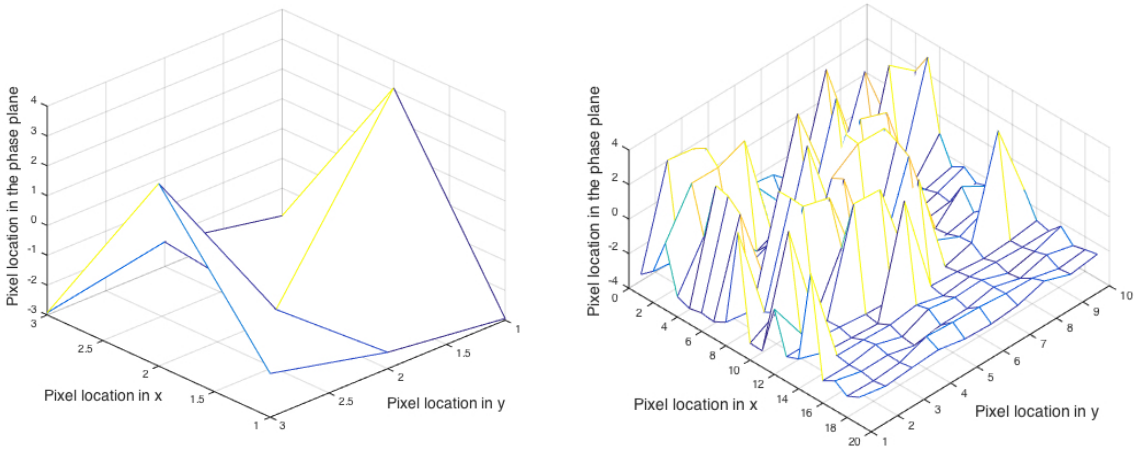

Figure 7: (Left) A specific 3-by-3 matrix from the region of interest displayed in figure 6. (Right) The entire region of interest from figure 6. Neither of these matrices display any of the traditional characteristics of a normal distribution

3-by-3 matrices are generally too small to determine the distribution of the dataset, however when the program expanded the size of the subsets of the image that it was extracting, the areas of interest it selected became less relevant, and were generally background noise or areas at the edge of the hand, where pixels of strong intensity intersected with pixels of low intensity. None of those selection points were accepted at the null-hypothesis when submitted to the multivariate Komogorov-Smirnov test.

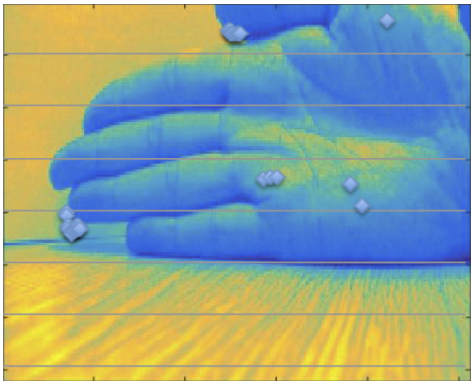

Figure 8: Regions best fit by a normal distribution, plotted over a down sampled colour map of the raw video file, which the program extracted while combing the phase map with 7-by-7 matrices.

3.3 Noise reductions in post-processed output

Initially, the datasets were analysed to determine the distribution of the noise. We found that the background noise in these datasets was unsurprisingly much more evenly distributed than in the full dataset, suggesting a 'salt and pepper' type of image noise. These distributions can be seen below in figure 9.

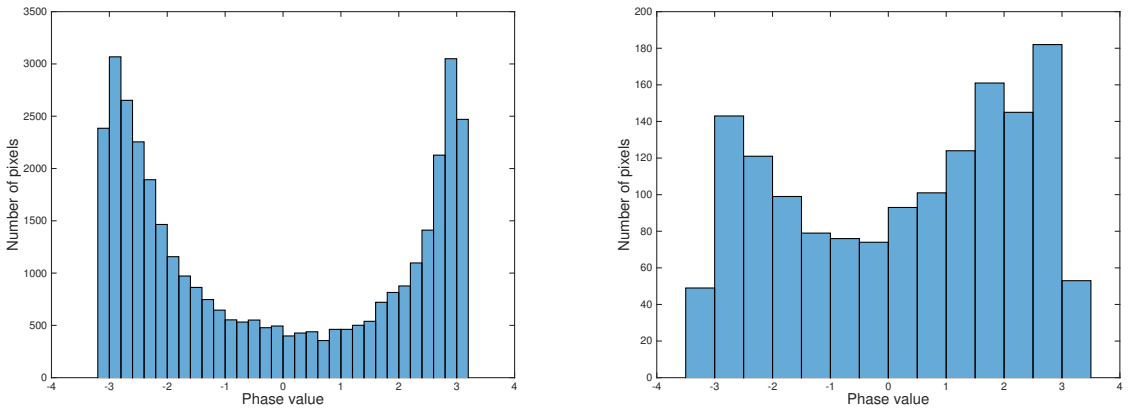

Figure 9: (Left) Histogram of phase values for all pixels in a dataset. (Right) Histogram of the phase values for pixels in a noisy background portion of the video.

This program was then applied to the same datasets as with the extraction of vital signs, and the blood perfusion distribution fitting. The program was run 3 times over the phase map, and successfully adjusted several outliers, without compromising the scope of the results. The resulting output, although not drastically different from an unaltered output, is nonetheless a cleaner image for the outlier filtering as can be seen in figure 10.

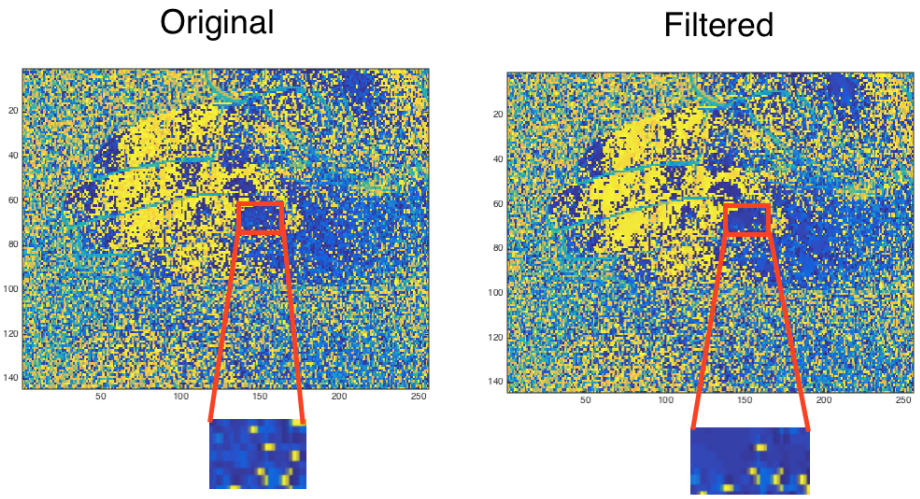

Figure 10: Original phase image versus the filtered phase image.

3.4 Patient results

The dataset recorded from the patient was 1280x720 pixels in size, 30 seconds long, and recorded at 60 fps. When we began to analyse the blood perfusion in the patient's dataset, we quickly realised that the patient's foot was moving in the video. This is likely to have been caused by a tremor that the patient was exhibiting. We believe that this tremor unfortunately lead to the program reproducing the pattern of the foot's movement, and not the blood perfusion. This is because the foot moved location in x and y, and so the pixel colour change that the video exaggerates to monitor perfusion, was actually just the movement of the patient's foot.

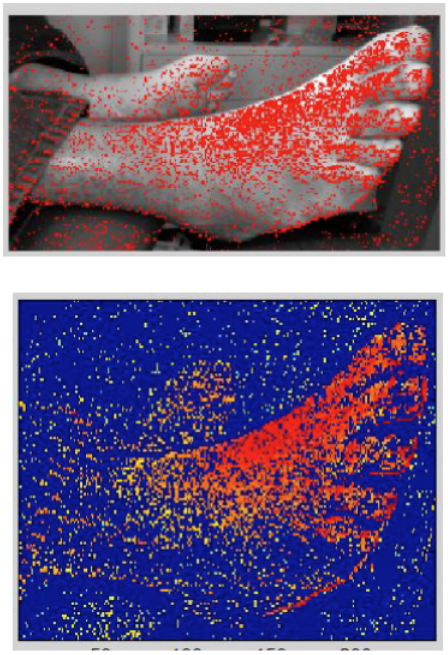

Figure 11: Blood perfusion output for the patient's foot. We believe this excellent reading to have actually been caused by the movement in their foot.

4 Discussion

4.1 Evaluation of post-processing techniques

The first technique that we presented, the objective locating of central points of perfusion through the fitting of distributions to matrix subsets, was unfortunately unsuccessful in its goals. We feel that the predominant issue with this technique, was its reliance on normal distributions for locating these central points of perfusion. This may be effective when looking at a flat skin surface, however for the vast majority of videos, these perfusion points may be better fit by a variety of other distributions. The initial 3-by-3 matrices did have some success in selecting areas of interest, but this was based on a small amount of data, and didn't effectively represent the complete image. A better approach to this issue may be through the use of machine learning algorithms that look for the characteristic features present in central points of perfusion, based upon a training set. One such technique that may be useful for this application would be cluster analysis, where the density of specific pixel sets could be used to classify whether the subset is characteristic of a central point of perfusion or not.

The second technique, outlier filtering, appeared to be successful in reducing outliers for the video output. The main issue with this filtering technique is that it indiscriminately reclassifies normal pixels, along with outlying pixels. This is a very difficult issue to overcome, and centres around the balance required between the tolerance range in the neighbouring pixels, and the amount of times that the program is looped through the perfusion video. Higher numbers of successive runs through the video, gives better outlier filtering, but also reclassifies higher amounts of non-outlying data, therefore altering any further analysis that may be conducted on the video. We don't feel that this is severe enough to compromise the overall blood perfusion results, however a different approach to removing noise in the image may be beneficial. One potential area for this, may be to focus on edge detection techniques to rapidly remove the background image, and therefore background noise, from the analysis.

4.2 How appropriate would the use of photoplethysmographic imaging be in a clinical setting?

The use of non-contact PPG imaging in a clinical setting has both positives and negatives associated with it. The clear benefit for its use, would be the simplicity of the setup. A low cost digital camera could be positioned over each hospital bed, providing a live feed of the patients vital signs, and blood perfusion through wounded areas, or areas of interest. This non-contact approach would not restrict the patient in their movement, or impair their rest, which is preferable over current contact based PPG methods, where the patient has wires attached to them. The growing variety of uses for non-contact PPG could also be implemented without additional equipment purchases. Any additional techniques could be implemented with software packages, and would be relatively low in cost. Regardless of these promising benefits, there are issues with the implementation of this technology. Predominantly, the unresolved issue of movement artefacts in non-contact PPG technology would be exhassebated by the constant video camera monitoring. The implementation of this technology would also likely raise concerns over patient data storage, and the function of algorithms for extended vital sign monitoring. For example, the technique must be able to detect changes in vital sign monitoring, and therefore a moving point average of heart rate frequencies must be utilised for the monitoring of vital signs, requiring modifications to the current non-contact PPG software that is used.

A useful test area for this technology may be in a hospital unit where patients must be continually monitored, but have little mobility or scope for movement. This may then inform the feasibility of this technique in a clinical setting whilst foregoing the vast array of potential issues arising from movement artefacts.

4.3 Directions for future research

Two potential directions for future research efforts in this field could be the improvement of motion detection in non-contact PPG setups, and the objective, automatic, detection of the heart rate frequency.

To begin with, the automatic detection of motion in PPG recordings could be exceptionally useful for preventing motion artefact noise, and vital sign false alarms. The algorithm could function through the monitoring of extreme changes in colouration of pixels. If the program detects an extreme colour change, then it could register this as a movement, stop analysing any PPG results, and wait for the extreme changes to stop for a certain amount of frames, before resuming the analysis that it was carrying out. Another direction for motion detection could be in the use of a marker that is placed on the patient, which the algorithm monitors for changing positions in x and y.

Secondly, an algorithm which can objectively search for the heart rate frequency would be exceptionally useful before the introduction of non-contact PPG imaging in a clinical setting. This algorithm could function by analysing the mean amplitude of peaks within a specific frequency range, and selecting the heart rate from that. Errors in this could arise from the accidental detection of a patient's respiration rate, or background noise. A strong implementation of this algorithm would need to feature some noise filtering to cancel these issues out.

5 Conclusion

In conclusion, we have attempted to evaluate the feasibility of using non-contact PPG technologies in a clinical setting based upon a broad literature review, and our own experience with the technique. In addition, we introduced two unique post-processing techniques with varying degrees of success for the analysis of non-contact PPG recordings, and have attempted to extract clinically relevant information from a patient dataset. The findings from both our patient dataset, and the post-processing techniques, gives directionality to future research, and highlights the issues of movement artefacts in non-contact PPG recordings.

References

[1] Kevin Y Woo, Vera Santos, and Monica Gamba. Understanding diabetic foot ulcers. *Nursing*, 43(10):36–42, Oct 2013.

[2] S Goodacre, F Sampson, M Stevenson, A Wailoo, A Sutton, S Thomas, T Locker, and A Ryan. Measurement of the clinical and cost-effectiveness of non-invasive diagnostic testing strategies for deep vein thrombosis. *Health Technol Assess*, 10(15):1–168, May 2006.

[3] Y A Wickramasinghe, L N Livera, S A Spencer, P Rolfe, and M S Thorniley. Plethysmographic validation of near infrared spectroscopic monitoring of cerebral blood volume. *Arch Dis Child*, 67(4 Spec No):407–411, Apr 1992.

[4] John Allen. Photoplethysmography and its application in clinical physiological measurement. *Physiol Meas*, 28(3):R1–39, Mar 2007.

[5] J W Severinghaus and J F Kelleher. Recent developments in pulse oximetry. *Anesthesiology*, 76(6):1018–1038, Jun 1992.

[6] P A Kyriacou. Pulse oximetry in the oesophagus. *Physiol Meas*, 27(1):R1–35, Jan 2006.

[7] Jyotirmoy Das, Amit Aggarwal, and Naresh Kumar Aggarwal. Pulse oximeter accuracy and precision at five different sensor locations in infants and children with cyanotic heart disease. *Indian J Anaesth*, 54(6):531–534, Nov 2010.

[8] P Lavoisier, R Barbe, and M Gally. Validation of a continuous penile blood-flow measurement by pulse-volume-plethysmography. *Int J Impot Res*, 14(2):116–120, Apr 2002.

[9] Y Iyriboz, S Powers, J Morrow, D Ayers, and G Landry. Accuracy of pulse oximeters in estimating heart rate at rest and during exercise. *Br J Sports Med*, 25(3):162–164, Sep 1991.

[10] R K Webb, A C Ralston, and W B Runciman. Potential errors in pulse oximetry. ii. effects of changes in saturation and signal quality. *Anaesthesia*, 46(3):207–212, Mar 1991.

[11] C C Y Poon and Y T Zhang. Cuff-less and noninvasive measurements of arterial blood pressure by pulse transit time. *Conf Proc IEEE Eng Med Biol Soc*, 6:5877–5880, 2005.

[12] B P Imholz, W Wieling, G A van Montfrans, and K H Wesseling. Fifteen years experience with finger arterial pressure monitoring: assessment of the technology. *Cardiovasc Res*, 38(3):605–616, Jun 1998.

[13] Youngzoon Yoon, Jung H Cho, and Gilwon Yoon. Non-constrained blood pressure monitoring using ecg and ppg for personal healthcare. *J Med Syst*, 33(4):261–266, Aug 2009.

[14] Marcel Azabji Kenfack, Federic Lador, Marc Licker, Christian Moia, Enrico Tam, Carlo Capelli, Denis Morel, and Guido Ferretti. Cardiac output by modelflow method from intra-arterial and fingertip pulse pressure profiles. *Clin Sci (Lond)*, 106(4):365–369, Apr 2004.

[15] Douglas Colquhoun, Lauren K Dunn, Timothy McMurry, and Robert H Thiele. The relationship between the area of peripherally-derived pressure volume loops and systemic vascular resistance. *J Clin Monit Comput*, 27(6):689–696, Dec 2013.

[16] Salvatore M Romano and Massimo Pistolesi. Assessment of cardiac output from systemic arterial pressure in humans. *Crit Care Med*, 30(8):1834–1841, Aug 2002.

[17] R Saxena, A Durward, N K Puppala, I A Murdoch, and S M Tibby. Pressure recording analytical method for measuring cardiac output in critically ill children: a validation study. *Br J Anaesth*, 110(3):425–431, Mar 2013.

[18] L Nilsson, A Johansson, and S Kalman. Monitoring of respiratory rate in postoperative care using a new photoplethysmographic technique. *J Clin Monit Comput*, 16(4):309–315, 2000.

[19] Lena M Nilsson. Respiration signals from photoplethysmography. *Anesth Analg*, 117(4):859–865, Oct 2013.

[20] Yu Sun, Sijung Hu, Vicente Azorin-Peris, Stephen Greenwald, Jonathon Chambers, and Yisheng Zhu. Motion-compensated noncontact imaging photoplethysmography to monitor cardiorespiratory status during exercise. *J Biomed Opt*, 16(7):077010, Jul 2011.

[21] F P Wieringa, F Mastik, and A F W van der Steen. Contactless multiple wavelength photoplethysmographic imaging: a first step toward "spo2 camera" technology. *Ann Biomed Eng*, 33(8):1034–1041, Aug 2005.

[22] Kenneth Humphreys, Tomas Ward, and Charles Markham. Noncontact simultaneous dual wavelength photoplethysmography: a further step toward noncontact pulse oximetry. *Rev Sci Instrum*, 78(4):044304, Apr 2007.

[23] Wim Verkruysse, Lars O Svaasand, and J Stuart Nelson. Remote plethysmographic imaging using ambient light. *Opt Express*, 16(26):21434–21445, Dec 2008.

[24] Ping Shi, Sijung Hu, Angelos Echiadis, Vicente Azorin Peris, Jia Zheng, and Yisheng Zhu. Development of a remote photoplethysmographic technique for human biometrics, 2009.

[25] Ming-Zher Poh, Nicholas C Swenson, and Rosalind W Picard. Motion-tolerant magnetic earring sensor and wireless earpiece for wearable photoplethysmography. *IEEE Trans Inf Technol Biomed*, 14(3):786–794, May 2010.

[26] Ming-Zher Poh, Daniel J McDuff, and Rosalind W Picard. Advancements in noncontact, multiparameter physiological measurements using a webcam. *IEEE Trans Biomed Eng*, 58(1):7–11, Jan 2011.

[27] B M Sayers. Analysis of heart rate variability. *Ergonomics*, 16(1):17–32, Jan 1973.

[28] He Liu, Yadong Wang, and Lei Wang. A review of non-contact, low-cost physiological information measurement based on photoplethysmographic imaging. *Conf Proc IEEE Eng Med Biol Soc*, 2012:2088–2091, 2012.

[29] Christopher G Scully, Jinseok Lee, Joseph Meyer, Alexander M Gorbach, Domhnull Granquist-Fraser, Yitzhak Mendelson, and Ki H Chon. Physiological parameter monitoring from optical recordings with a mobile phone. *IEEE Trans Biomed Eng*, 59(2):303–306, Feb 2012.

[30] Yunyoung Nam, Jinseok Lee, and Ki H Chon. Respiratory rate estimation from the built-in cameras of smartphones and tablets. *Ann Biomed Eng*, 42(4):885–898, Apr 2014.

[31] Frederic Bousefsaf, Choubeila Maaoui, and Alain Pruski. Remote detection of mental workload changes using cardiac parameters assessed with a low-cost webcam. *Comput Biol Med*, 53:154–163, Oct 2014.

[32] L Tarassenko, M Villarroel, A Guazzi, J Jorge, D A Clifton, and C Pugh. Non-contact video-based vital sign monitoring using ambient light and auto-regressive models. *Physiol Meas*, 35(5):807–831, May 2014.

[33] Lonneke A M Aarts, Vincent Jeanne, John P Cleary, C Lieber, J Stuart Nelson, Sidarto Bambang Oetomo, and Wim Verkruysse. Non-contact heart rate monitoring utilizing camera photoplethysmography in the neonatal intensive care unit - a pilot study. *Early Hum Dev*, 89(12):943–948, Dec 2013.

[34] M Sandberg, Q Zhang, J Styf, B Gerdle, and L-G Lindberg. Non-invasive monitoring of muscle blood perfusion by photoplethysmography: evaluation of a new application. *Acta Physiol Scand*, 183(4):335–343, Apr 2005.

[35] R. Erts, U. Rubins, and J. Spigulis. Monitoring of blood pulsation using non-contact technique. *IFMBE Proceedings*, 25(4):754–756, 2005.

[36] Jia Zheng, Sijung Hu, Angelos S. Echiadis, Vince Azorin-Peris, Ping Shi, and Vasilios Chouliaras. A remote approach to measure blood perfusion from the human face, 2009.

[37] U. Rubins, R. Erts, and V. Nikiforovs. The blood perfusion mapping in the human skin by photoplethysmography imaging. *XII Mediterranean Conference on Medical and Biological Engineering and Computing 2010*, 29:304–306, 2010.

[38] Hao-Yu Wu, Michael Rubinstein, Eugene Shih, John Guttag, Fredo Durand, and William Freeman. Eulerian video magnification for revealing subtle changes in the world. *ACM Transactions on Graphics*, 31(4), 2012.

[39] Armando Rosales-Velderrain, Michael Padilla, Charles H Choe, and Alan R Hargens. Increased microvascular flow and foot sensation with mild continuous external compression. *Physiol Rep*, 1(7):e00157, Dec 2013.

[40] Nina Zaproudina, Victor Teplov, Ervin Nippolainen, Jukka A. Lipponen, Alexei A. Kamshilin, Matti Närhi, Pasi A. Karjalainen, and Rashid Giniatullin. Asynchronicity of facial blood perfusion in migraine. *PLoS ONE*, 2013.

[41] Nikolai Blanik, Abbas K Abbas, Boudewijn Venema, Vladimir Blazek, and Steffen Leonhardt. Hybrid optical imaging technology for long-term remote monitoring of skin perfusion and temperature behavior. *J Biomed Opt*, 19(1):16012, Jan 2014.

[42] Mike Sheppard. All fit distribution, January 2015.

[43] Liran Carmel. Multivariate analysis toolbox for matlab, January 2015.

[44] Ana Justel, Daniel Pena, and Ruben Zamar. A multivariate kolmogorov-smirnov test of goodness of fit. *Statistics and Probability Letters*, 35:251–259, January 1997.

[45] Rangachar Kasturi and Brian G. Schunck. *Machine Vision*, volume 1 of *McGraw-Hill Series in Computer Science*. McGraw-Hill Science/Engineering/Math, 1st edition, 1995.